Annals of Science and Technology - A, Vol 9 (2): 11-30, 2024

ISSN: 2 544 6320

ARTICLE

Dual Approach Evaluation of Vildagliptin-Metformin Conjugate and Silymarin as Antioxidants against Doxorubicin Toxicity: *In Silico* and *In Vitro* Studies

Adejuwon A. Adeneye*[1,2], Mariam O. Amuni[1]

[1]*Department of Pharmacology, Therapeutics and Toxicology, Faculty of Basic Clinical Science, Lagos State University College of Medicine, Ikeja, Lagos State, Nigeria*
[2]*Directorate of Research Management and Innovation, Office of the Vice Chancellor, Babatunde Raji Fashola Senate Building, Lagos State University, Main Campus, Ojo, Lagos State, Nigeria*

Received 15th January 2024, Accepted 11th July, 2024
DOI: 10.2478/ast-2024-0005

**Corresponding author*
Adejuwon Adewale ADENEYE (MBBS, PhD, DSc). E-mail: adejuwon.adeneye@lasucom.edu.ng; Tel: +2348035835589

Abstract
Doxorubicin, a potent and common anthracycline antibiotic used in cancer treatment, is limited by its severe off-target, multi-organ toxicities. This study investigates the protective effects and underlying mechanisms of metformin, vildagliptin, vildagliptin-metformin conjugate, and silymarin against doxorubicin-induced toxicities. Molecular docking studies were conducted to assess the interaction of these compounds with key protein targets involved in apoptosis (Bax, caspase-3, CXCR1), oxidative stress (catalase, glutathione reductase), and vascular endothelial damage (VCAM-1). Additionally, *in vitro* antioxidant activities were evaluated using DPPH, NO, and FRAP assays. Metformin showed potential through Bax and catalase pathways, vildagliptin through caspase-3, CXCR1, and catalase pathways, and silymarin through caspase-3, catalase, and VCAM-1 pathways. The vildagliptin-metformin conjugate exhibited combined protective mechanisms, suggesting a strong therapeutic potential. The binding affinities of these compounds to their respective targets surpassed doxorubicin, indicating their ability to either displace or inhibit doxorubicin binding. Thus, this study highlights vildagliptin-metformin conjugate and silymarin as promising adjuvants for mitigating doxorubicin-induced toxicities.

Keywords: Doxorubicin Toxicity; Molecular Docking; *In vitro* Antioxidant Assays; Vildagliptin-Metformin Conjugate; Apoptosis Pathways; Silymarin

1.0 Introduction

Doxorubicin, sold under the brand name "Adriamycin", is an anthracycline antibiotic cytotoxic that is often used in the clinical management of both solid, soft tissue, as well as hematological tumors since its approval for medical use by the United States Food and Drug Administration (FDA) in 1974 (Fukuda et al., 2017; Tian et al., 2020; Lee et al., 2023, Wang et al., 2024). However, its use is limited by its off-target organ toxicities that are attributed to its free radicals generation (Li et al., 2022). The main reason behind the toxicity is the free radicals generation with preponderance for the heart first and followed by the liver, kidneys, ovaries and testes, adipose tissue, and brain in that order (Rivankar, 2014; Ranu et al., 2022).

The various drugs for the possible antidotal activities against doxorubicin-induced toxicities include dexrazoxane (Levi et al., 2015), carnosine (Caruso et al., 2022), visnagin (Asnani et al., 2018), silymarin (Rašković et al., 2011), *Clerodendrum volubile* (Olorundare et al., 2020), dimethyl sulfoxide (DMSO) (Pérez Fidalgo et al., 2012). Even though dexrazoxane remains the only FDA-approved drug for the treatment of doxorubicin cardiomyopathy, its clinical use is still associated with some limitations (Chen et al., 2022). Hence, the need to find other effective therapeutic drugs becomes inevitable. Also, previous studies have reported metformin (Asensio-López et al., 2011; Zilinyi et al., 2018; Ajzashokouhi et al., 2020; Agaba et al., 2021; Van et al., 2023) and its different fixed-dose combinations such as metformin and dapagliflozin (Satyam et al., 2023), metformin-sitagliptin (Kelleni et al., 2015; Sheta et al., 2016) to effectively mitigated doxorubicin-induced cardiotoxicity in Wistar rats (Renu et al., 2022). Therefore, this study investigated the potential role and the underlying mechanisms of action of metformin, vildagliptin, vildagliptin-metformin conjugate, and silymarin in ameliorating doxorubicin-associated toxicities using molecular docking to study the ligand-protein target interactions and *in vitro* antioxidant studies.

2.0 Experimental

2.1. Protocol for the Blind Molecular Docking of the test drugs (metformin, vildagliptin, vildagliptin-metformin fixed dose combination (®GalvusMet) and silymarin

2.1.1. Retrieval and Preparation of Target Protein Crystal Three-Dimensional Structure

The three-dimensional crystal structure of each specified target (as detailed in Table 1) was obtained from the RCSB Protein Database (https://www.rcsb.org/pdb/home/home.do). Subsequently, the structures were processed using the PyMol toolkit, involving the removal of non-essential water molecules and all heteroatoms. Simultaneously, the coordinates for the protein binding pocket grid were automatically defined using PyRx AutoDock Vina (Trott and Olson, 2010).

2.1.2. Retrieval and Preparation of Study Ligands

The chemical structure description files for silymarin (PubChem ID: 5213), metformin (PubChem ID: 4091), vildagliptin (PubChem ID: 6918537), and their respective standard inhibitors or activators, as outlined in Table 1 were retrieved from the NCBI PubChem database (https://pubchem.ncbi.nlm.nih.gov/). Vildagliptin-metformin complex was formed through conjugation by using the Schrodinger merger tool. Subsequently, the acquired ligands underwent conversion from MOL SDF format to PDBQT files using open Babel integrated into the PyRx tool, facilitating the generation of atomic coordinates. Ligand energy minimization, which involved the addition of Kohlmann and Gasteiger charges, was performed using the PyRx Open Babel optimization algorithm with the force field set to the universal force field (UFF) as required in PyRx (Trott and Olson, 2010).

2.1.3. Blind Molecular Docking Protocol for Test Drugs (metformin, vildagliptin, vildagliptin-metformin fixed dose combination and silymarin

The blind molecular docking analysis of ligands within the receptor was executed by utilizing the PyRx AutoDock Vina exhaustive search anchoring algorithm. This approach incorporated notation functions derived from the Nelder-Mead-Simplex algorithm, applied across diverse grid resolution coordinates as per the reduction procedure outlined by Trott and Olson (2010).

2.1.4. Protein-Ligand Binding Affinity Calculations and Interaction Visualization

The initial step involved anchoring the default standard ligands (as indicated in **Table 1**) within the corresponding protein binding site. Subsequently, its interaction with the study compounds was compared at the same active sites, employing identical grid box dimensions. Docking results were visually depicted through scatter plots and visualized using Osiris Data Warrior version 5.5.0 (López-López et al., 2019).

For a detailed examination, the interaction of each ligand with the target binding pocket and their three-dimensional (3D) interactions with the target residues were visualized. This

visualization was conducted using the Python Molecular Graphics Interface (PyMol®) version 2.2.0 software (Du et al., 2016). The hydrophobic nature of interactions between ligand atoms and target active residues, along with their two-dimensional interactions, was analyzed using BIOVIA Discovery Suite version 17.2.0.16349 (Baroroh et al., 2023). In this study, the optimal binding pose at the target binding site was determined based on the local minimum energy conformation binding mode of the compounds (Du et al., 2016).

2.2. Determination of In Vitro Antioxidant Activities of metformin, vildagliptin, vildagliptin-metformin fixed dose combination, silymarin and ascorbic acid

2.2.1. Determination of 1,1, dipheny-2-picrylhydrazyl (DPPH) Radical Scavenging Activities

The DPPH radical scavenging assay was performed using 1,1 diphenyl-2-picrylhydrazyl (DPPH) according to the method described by Brand-Williams et al. (1995) with some modifications (Guchu et al., 2020). Briefly described, four different concentrations of the studied drugs (25, 50, 75 and 100 µg/ml) were prepared in methanol (analytical grade). The same concentrations were also prepared for L-ascorbic acid, which was used as a standard antioxidant. 1 ml of each studied extract was transferred into a clean test tube into which 0.5 ml of 0.3 mM DPPH in methanol was added. The mixture was shaken and left to stand in the dark at room temperature for 15 minutes. Blank solutions comprising of the studied extract solutions (2.5 ml) and 1 ml of methanol were used as baseline.

The negative control comprised 2.5 ml of DPPH solution and 1 ml of methanol, while L-ascorbic acid at the same concentrations as the studied extracts was used as the positive control. After incubation in the dark, the absorbance values were measured at 517 nm using a spectrophotometer. The experiments were performed in quadriplicate.

Percentage DPPH radical scavenging activity was calculated by the following equation:

% DPPH radical scavenging activity = {(Ab − Ad) ÷ Ab}× 100

where As is the absorbance of the control (blank solution), and Ad is the absorbance of the tested drugs/standard. Then the percentage (%) of inhibition was considered.

2.2.2. Ferric Reducing Antioxidant Power Assay

The reducing powers of metformin, vildagliptin, vildagliptin-metformin fixed dose combination, silymarin and ascorbic acid were determined according to the method described by Oyaizu (1986) and Guchu et al. (2020), with some modifications. Briefly described, four different concentrations of each of the drugs (0.25, 0.50, 0.75 and 100 µg/ml) and L-ascorbic acid at same concentrations were mixed with 2 ml phosphate buffer (0.2 M, pH 6.6) and 2 ml of 1% potassium ferricyanide ($K_3Fe(CN)_6$). The mixture was incubated at 50°C for 20 minutes. Then, 2 ml of 10% trichloroacetic acid (TCA) was added, and the mixture was centrifuged at 1000 revolutions per minute (rpm) for 10 min. Two milliliter (2ml) of the supernatant was aspirated and mixed with 2 ml of distilled water and 1 ml of 0.1% ferric chloride ($FeCl_3$). In each case, the experiment was performed in quadriplicate. Afterward, the absorbances were measured spectrophotometrically at 700 nm using a UV-spectrophotometer against blank and recorded. Increased absorbance of the reaction mixture indicates increased reducing capacity. The experiment was repeated in quadriplicate times at each concentration.

2.2.3. Nitric Oxide Radical Scavenging Assay

The nitric oxide radical scavenging assay was conducted using the methods described by Adebayo et al. (2019) and Chelliah et al. (2022). The test drugs (metformin, vildagliptin, vildagliptin-metformin fixed dose combination, silymarin and ascorbic acid) were prepared from a 1 mg/ml solution. These were then serially diluted with distilled water to make concentrations from 25, 50, 75 and 100 µg/ml of the tested drugs and the standard ascorbic acid. These were stored at 4°C for later use. Griess reagent was prepared by mixing equal amounts of 1% sulphanilamide in 2.5% phosphoric acid and 0.1% naphthylethylene diamine dihydrochloride in 2.5% phosphoric acid immediately before use. A volume of 0.5 mL of 10 mM sodium nitroprusside in phosphate buffered saline was mixed with 1 ml of the different concentrations of the tested drugs (25-100 µg/ml) and incubated at 25°C for 180 min. The solution was mixed with an equal volume of freshly prepared Griess reagent. The blank solution with an equal volume of buffer were prepared in a similar manner as was done for the test samples. The colour tubes contained the tested drugs at the same concentrations with no sodium nitroprusside. A volume of 150 µl of the reaction mixture was transferred to a 96-well plate. The absorbance was measured at 546 nm using a SpectraMax Plus UV-Vis microplate reader (Molecular Devices, GA, USA). Ascorbic acid was used as the positive control. The percentage inhibition of the extract and standard was calculated and recorded. The percentage nitrite radical scavenging activity of the tested drugs and ascorbic acid were calculated using the following formula:

% nitrite radical scavenging activity = {(Ab − Ad) ÷ Ab} × 100

where Ab = absorbance of the blank solution and Ad = absorbance of the tested drugs/standards.

2.3. Statistical Analysis

The quantitative data were presented in tables, while the exported data were analyzed using GraphPad Instat software version 5.0 (GraphPad Prism Inc., San Diego, CA, USA). The data were subjected to descriptive statistics and stated as mean ± standard error of the mean (SEM). One-way analysis of variance (ANOVA) was used in analyzing for significant differences in the means within and between the different treatment groups, followed by Tukey's tests for pairwise comparisons and separation of means. In the molecular docking studies, the hydrophobic interactions between ligand atoms and target active residues, along with their two-dimensional interactions, were analyzed using BIOVIA Discovery Suite Visualizer, version 17.2.0.16349 (Dassault Systèmes, Vélizy-Villacoublay, France) as described by Du et al. (2016). The local minimum energy conformation binding mode for each tested compound is regarded as the optimal binding pose at the target binding site in the study (Peach et al., 2020).

Results and Discussion

3.1. In silico computational studies on the possible pathway binding proteins of metformin, vildagliptin, vildagliptin-metformin fixed dose combination and silymarin

3.1.1. Binding activities of metformin, vildagliptin, vildagliptin-metformin fixed dose combination and silymarin on BCL-2 associated X protein

The various docked drugs except silymarin (5.6 kcal/mol) displayed relatively higher binding affinities than MSN-125 (4.4 kcal/mol) as the standard BAX protein inhibitor (Table 2). The active pocket residues of BAX protein obtained on the PrankWeb-based algorithm are: A_111, A_114, A_158, A_161, A_162, A_165, A_23, A_26, A_27, A_59, A_62, A_63, and A_66.

The break down to the binding interactions of the different docked drugs are as thus provided:

3.1.1.1. The binding interaction of metformin with the BCL-2 associated X protein

Metformin binds to the side chain residue GLN 32, ASP 48, and SER 60 that are proximally close to the protein active pocket, respectively, through the conventional hydrogen bond, attractive charge, and carbon-hydrogen bond at the average bond distances of 2.40 Å, 3.85 Å, and 3.79 Å with less hydrophobicity revolving around the interactions (Figures 1a and 1b).

3.1.1.2. The binding interaction of vildagliptin with the BCL-2 associated X protein

Vildagliptin binds with the closely proximal side chain residues MET 20, LYS 21, and ALA 24 of the BAX protein through the hydrophobic alkyl bond at the average bond distances of 4.69 Å, 4.42 Å, and 4.28 Å, with the relatively high hydrophobicity of interactions concentrating around the ALA 24 binding (Figures 2a and 2b).

3.1.1.3. The binding interaction of vildagliptin-metformin conjugate with the BCL-2 associated X protein

The vildagliptin-metformin conjugate binds to the side chain hinge residues of MET 137 in addition to proximal side chain residues LEU 47, ALA 24, and MET 20 of the BAX protein through the hydrophobic alkyl bond at the average bond distances of 4.58 Å, 5.27 Å, 4.73 Å, respectively, as well as LYS 21 through the conventional hydrogen bond at the average bond distance of 3.96 Å while the relatively hydrophobicity values of interactions revolve around the ALA 24, LEU 47, and MET 20 binding (Figures 3a and 3b).

3.1.1.4. The binding interaction of MSN-125 with the BCL-2 associated X protein

MSN-125, the standard BAX protein inhibitor, binds to the active binding pocket residues CYS 62, ILE 66, LEU 63, LEU 59, PHE 165, LEU 161, and VAL 111 of the BAX protein, respectively, through the hydrophobic alkyl, Pi-Sigma, Pi-Alkyl, Pi-Sigma at the average bond distances of 5.14 Å, 4.71 Å, 3.25 Å, 5.03 Å, 4.13 Å, 5.03 Å, 3.66 Å, in addition to LEU 27 which binds to the compound conjugate through the conventional hydrogen bond at the bond distance of 2.67 Å. That is in addition to binding to side chain residues LEU 70, VAL 177, ALA 112, as well as ARG 65 through the hydrophobic alkyl bond and amide-Pi-stacked bond at the bond distances of 5.33 Å, 4.11 Å, 3.45 Å, and 4.48 Å (Figures 4a and 4b).

The fact that all docked drugs except silymarin displayed relatively higher binding affinities than the standard Bax inhibitor, MSN-125, showed that these drugs strongly bind and negate the inhibitory active of MSN-125, thereby mediating their anti-apoptotic effect via Bax pathways (Figures 4a and 4b). This report is in complete agreement with previous studies that showed that metformin elicited anti-apoptosis Bax/Bcl-2 pathways in rats (El Kiki et al., 2020).

3.1.2. Binding activities of metformin, vildagliptin, vildagliptin-metformin fixed dose combination and silymarin on caspase-3 protein

Silymarin (-7.5 kcal/mol), among the docked compounds, exhibited relatively higher binding affinities than VRT-043198 (the standard inhibitor) (-6 kcal/mol) for caspase-3 while the vildagliptin-metformin conjugate compound exhibited

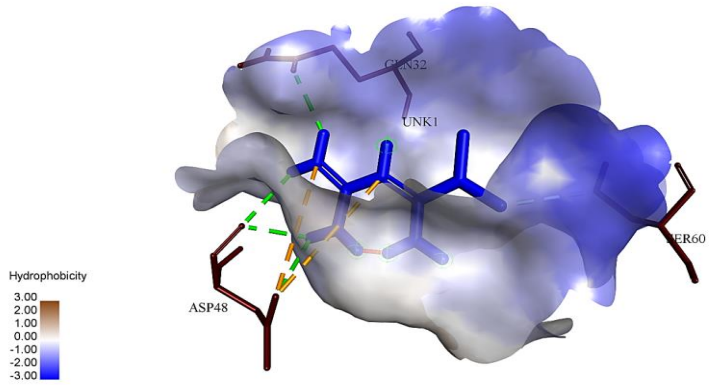

Figure 1a. Pocket hydrophobicity view of the interaction between metformin and BCL-2-associated X protein

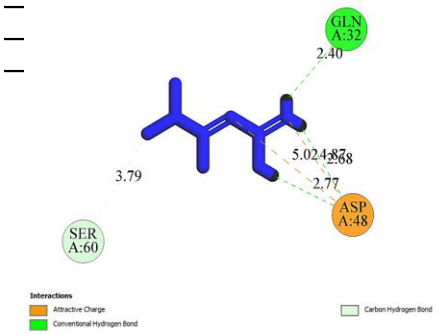

Figure 1b. Two-dimensional view of the interaction between metformin and BCL-2-associated X Protein

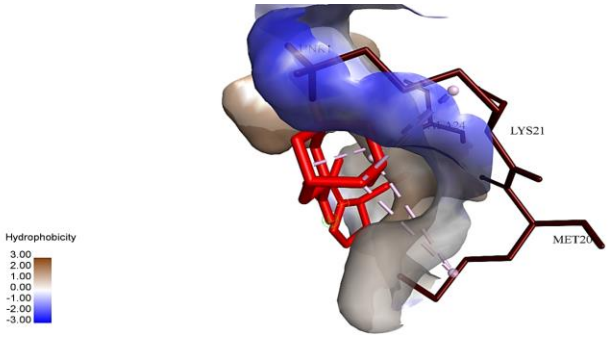

Figure 2a. Pocket hydrophobicity view of interaction between vildagliptin and BCL-2-associated X Protein

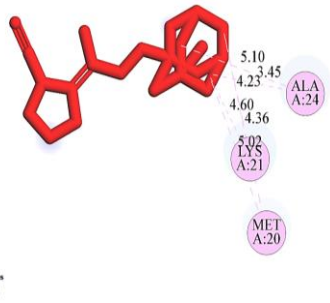

Figure 2b. Two-dimensional view of the interaction between vildagliptin and BCL-2-associated X Protein

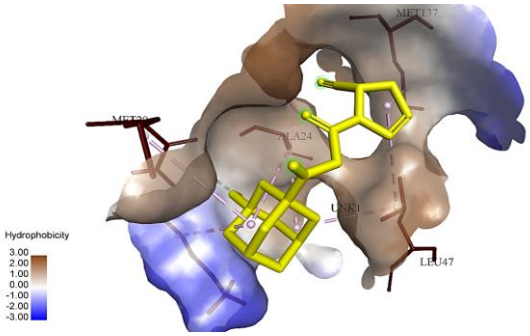

Figure 3a. Pocket hydrophobicity view of the interaction between vildagliptin-metformin conjugate and BCL-2-associated X Protein

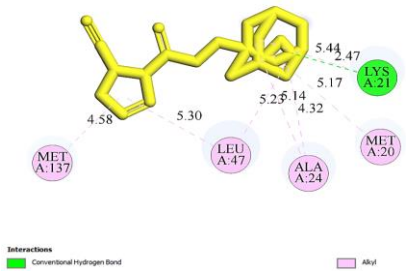

Figure 3b. Two-Dimensional view of the interaction between vildgaliptin-metformin conjugate and BCL-2-associated X Protein

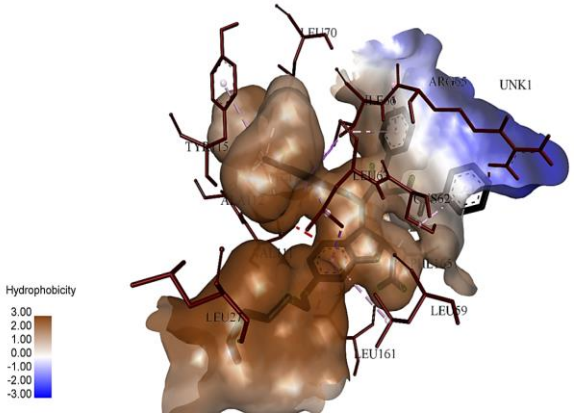

Figure 4a. Pocket hydrophobicity view of the interaction between MSN-125 and BCL-2-associated X Protein

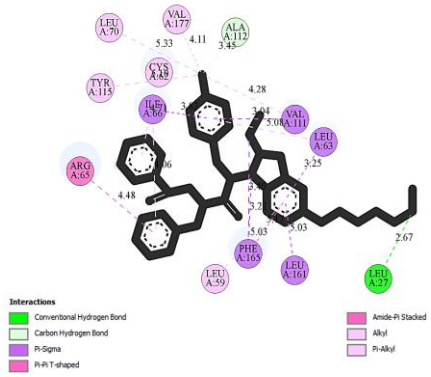

Figure 4b. Two-Dimensional view of the interaction between MSN-125 and BCL-2-associated X Protein

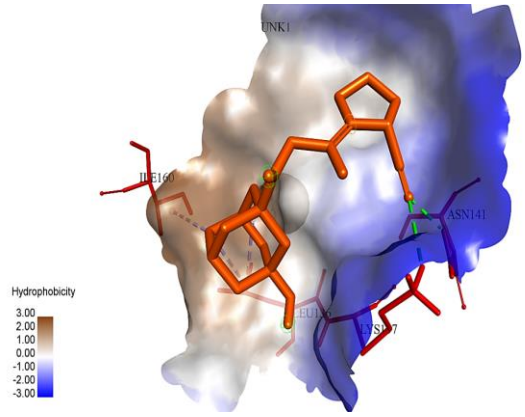

Figure 5a. Pocket hydrophobicity view of interaction between silymarin and caspase 3

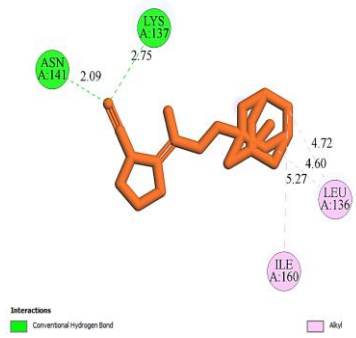

Figure 5b. Two-dimensional view of the interaction between silymarin and caspase 3

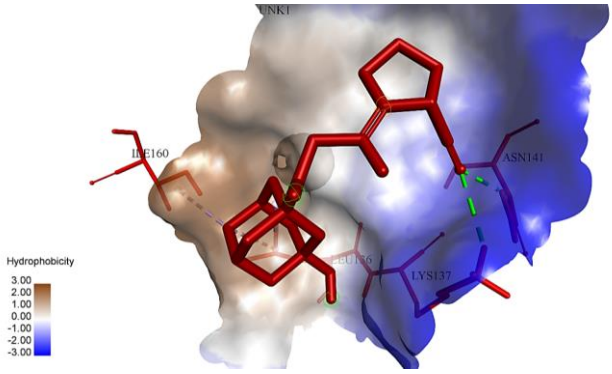

Figure 6a. Pocket hydrophobicity view of the interaction between vildagliptin and caspase-3

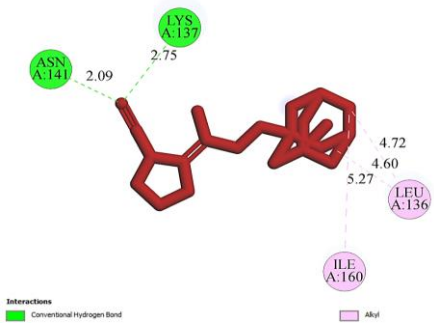

Figure 6b. Two-dimensional view of the interaction between vildagliptin and caspase-3

Table 1: Study Targets and their Corresponding Standard Modulators

Target Protein	**Protein Data Bank Identification Code (PDB ID)**	**Gene Source**	**Standard Ligand/Type**
BCL-2-associated X Protein (BAX)	MSN-125	*Homo sapiens*	MSN-125/I*
Caspase 3	3KJF	*Homo sapiens*	VRT-043198/I*
Catalase	Human erythrocyte catalase 3-amino-1,2,4-triazole complex (1DGH)	*Homo sapiens*	Metformin/A*
Glutathione Reductase	1GRE	*Homo sapiens*	Oxiglutathione/A*
Vascular Cell Adhesion Molecule 1 (VCAM 1)	Varacin-1 (VCA-1)	*Homo sapiens*	BDBM50105195/I*
C-X-C Motif Chemokine Receptor 1 (CXCR1)	2LNL	*Homo sapiens*	Reparixin/I*

I* - Inhibitor; A* - Activator

Table 2: The binding affinity of metformin, vildagliptin, vildagliptin-metformin fixed dose combination (GalvusMet®), silymarin and standard ligands (agonists/inhibitors) to the pathways in doxorubicin toxicities.

Binding affinity (kcal/mol)	Tested Drugs				
	MET	VIL	VIL-MET	SIL	STL
BCL-2	-4.6	-4.8	-4.7	+5.6	+4.4 (MSN-125)
BCL-2	-4.2	-6.0	-5.6	-7.5	-6.0 (VRT-043198)
CAT	-5.2	-8.8	-9.1	-12.4	-
GR	-5.2	-7.4	-7.2	-9.4	-7.0 (Oxiglutathione)
VCAM-1	-4.2	-6.5	-6.4	-6.5	-5.6 (BDBM50105195)
CXCR1	-5.1	-8.8	-8.8	-4.5	-7.9 (Reparixin)

BCL-2 - BCL-2 associated X Protein, CAT - catalase, GR - glutathione reductase,
VCAM-1 - vascular cell adhesion molecule-1, CXCR1 - C-X-C chemokine receptor-1, MET - metformin, VIL - vildgaliptin, VIL-MET - vildagliptin-metformin conjugate, SIL - silymarin, STL - standard ligands

Table 3: Scavenging effect of metformin, vildagliptin, vildagliptin-metformin fixed dose combination (GalvusMet®), silymarin and ascorbic acid on DPPH radicals

	%free radical scavenging activities at different concentrations				
	25µg/ml	50µg/ml	75µg/ml	100µg/ml	IC_{50} (µg/ml)
MET	45.76±0.27	51.35±0.27^{a+}	57.88±0.40^{b+}	66.59±1.12$^{c+,c\S}$	43.96±0.30^{e}
VIL	36.90±0.40	41.68±0.24^{a+}	60.21±0.14^{b+}	64.59±0.27$^{c+,c\S}$	61.23±0.48
VM	37.18±0.14	53.84±0.15^{b+}	61.93±0.20^{b+}	77.26±0.05^{c+}	44.24±0.14^{e}
SIL	53.20±0.24	56.01±0.40	63.36±0.34^{a+}	83.90±0.27$^{c+,a\S}$	31.87±0.31^{f}
AA	54.02±0.42	65.90±0.10	78.97±0.16^{b+}	84.34±0.10^{c+}	29.84±0.17^{f}

MET - Metformin, VIL - vildagliptin, VM - vildagliptin-metformin fixed dose combination, SIL - silymarin, AA - ascorbic acid
$^{a+, b+}$ and $^{c+}$ represent significant increases at p<0.05, p<0.001 and p<0.0001, respectively, when compared to the 25µg/ml concentration values while ^{a§} and ^{c§} represent significant decreases at p<0.05 and p<0.0001, respectively when compared to AA values
^{e} and ^{f} represent significant inhibitions at p<0.01 and p<0.001, respectively, when compared to VIL value.

equivalent binding affinity with the standard for caspase-3 (-6 kcal/mol) (Table 2). The active pocket residues of caspase-3 protein based on the PrankWeb-based algorithm included A_120, A_121, A_122, A_123, A_128, A_161, A_162, A_163, A_165, A_166, A_61, A_62, A_63, A_64, and A_65.

3.1.2.1. The binding interaction of silymarin with the caspase 3 protein

Silymarin binds to the side-chain residues ASN 141, and LYS 137 of the caspase-3 protein through the conventional hydrogen bond at the average distances of 2.09 Å, 2.75 Å, respectively, and proximal side-chain residues ILE 160; LEU 136 through the hydrophobic alkyl bond at the average distances of 5.27 Å, and 5.16 Å, respectively, with the relatively high hydrophobicity of the interactions concentrating around the ILE 160 binding (Figures 5a and 5b).

3.1.2.2. The binding interaction of vildagliptinin with the caspase 3 protein

Vildagliptin binds to the side chain residues ASN 141, and LYS 137 of the caspase-3 protein through the conventional hydrogen bond at the average distances of 2.09 Å; 2.75 Å, respectively, and proximal side chain residues ILE 160, LEU 136 through the hydrophobic alkyl bond at the average distances of 5.27 Å and 5.16 Å respectively, with the relatively high hydrophobicity of the interactions concentrating around the ILE 160 binding (Figures 6a and 6b).

Table 4: Scavenging effect of metformin, vildagliptin, vildagliptin-metformin fixed dose combination, silymarin and ascorbic acid via FRAP assay

	% FRAP activities at different concentrations				
	25µg/ml	50µg/ml	75µg/ml	100µg/ml	IC_{50} (µg/ml)
MET	15.06±0.69	21.17±0.14^{a+}	47.60±0.61^{b+}	62.34±0.50$^{c+,c§}$	79.07±0.49^{d}
VIL	14.10±0.56	23.30±0.24^{a+}	42.55±0.73^{b+}	52.5±0.00$^{c+,c§}$	93.72±0.38
VM	14.62±0.20	22.65±0.11^{b+}	53.67±0.02^{b+}	68.31±0.38$^{c+,c§}$	72.04±0.43^{e}
SIL	15.30±0.21	22.83±0.40^{a+}	58.91±0.07^{c+}	70.35±0.10$^{c+,c§}$	68.83±0.20^{f}
AA	18.10±0.34	31.67±0.35^{a+}	67.25±0.05^{c+}	74.50±0.30^{c+}	62.88±0.26^{f}

MET - Metformin, VIL - vildagliptin, VM - vildagliptin-metformin fixed dose combination, SIL - silymarin, AA - ascorbic acid
$^{a+, b+}$ and $^{c+}$ represent significant increases at p<0.05, p<0.001 and p<0.0001, respectively, when compared to the 25µg/ml concentration values while ^{c§} represents a significant decrease at p<0.05 and p<0.0001, respectively when compared to AA values
$^{d, e}$ and ^{f} represent significant inhibitions at p<0.05, p<0.01 and p<0.001, respectively, when compared to VIL value.

Table 5: Nitrite radical scavenging activity of metformin, vildagliptin, vildagliptin-metformin fixed dose combination (GalvusMet®), silymarin and ascorbic acid

	% Free radical scavenging activities at different concentrations				
	25µg/ml	50µg/ml 75µg/ml		100µg/ml	IC_{50} (µg/ml)
MET	40.16±0.12	47.47±0.20^{a+}	53.77±0.18^{b+}	55.40±0.10$^{b+,c§}$	60.04±0.15
VIL	39.52±0.16	46.37±0.12^{a+}	53.87±0.16^{b+}	58.48±0.22$^{c+,c§}$	62.10±0.11
VM	40.17±0.12	47.88±1.08^{a+}	63.74±0.16^{c+}	70.89±0.36^{c+}	53.34±0.43^{d}
SIL	45.87±0.16	50.36±0.24	57.09±0.09^{b+}	76.88±0.12$^{c+,a§}$	48.00±0.15^{d}
AA	45.93±0.33	59.45±0.25^{b+}	73.55±0.51^{c+}	85.76±0.34^{c+}	32.53±0.36^{e}

MET - Metformin, VIL - vildagliptin, VM - vildagliptin-metformin fixed dose combination, SIL - silymarin, AA - ascorbic acid
$^{a+, b+}$ and $^{c+}$ represent significant increases at p<0.05, p<0.001 and p<0.0001, respectively, when compared to the 25µg/ml concentration values while ^{a§} and ^{c§} represent significant decreases at p<0.05 and p<0.0001, respectively when compared to AA values
^{d} and ^{e} represent significant inhibitions at p<0.05 and p<0.01, respectively, when compared to either MET or VIL value.

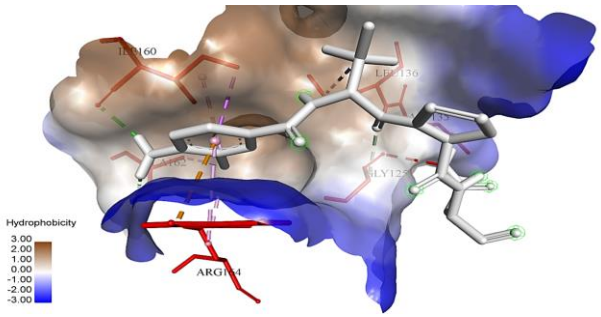

Figure 7a. Pocket hydrophobicity view of the interaction between VRT-043198 and caspase-3 protein

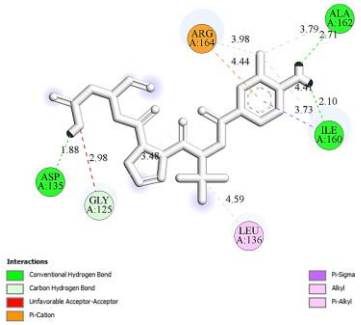

Figure 7b. Two-dimensional view of the interaction between VRT-043198 and caspase-3 protein

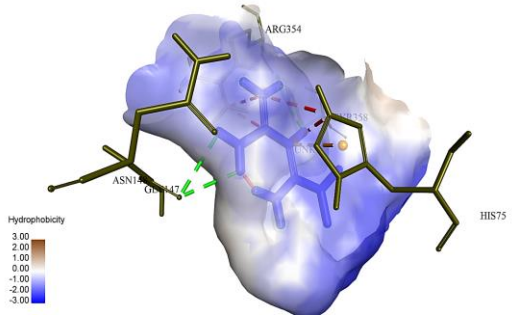

Figure 8a. Pocket hydrophobicity view of the interaction between metformin and catalase

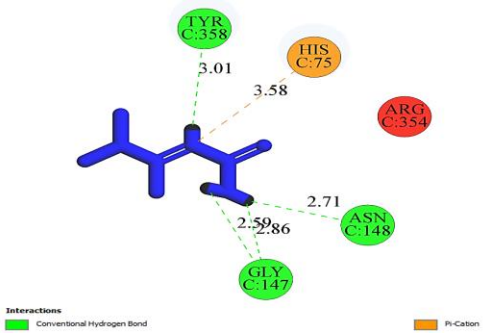

Figure 8b. Two-dimensional view of the interaction between metformin and catalase

3.1.2.3. The binding interaction of VRT-043198 with the caspase-3 protein

The standard caspase-3 inhibitor (VRT-043198) binds to the side chain residues in proximity to the active pockets including LEU 136, ARG 164, GLY 125, ASP 135, and ILE 160 of the caspase-3 protein through the hydrophobic Pi-Alkyl bond, Pi-cation bond, carbon-hydrogen bond, and conventional hydrogen bond at the bond distances of 4.59 Å, 4.21 Å, 2.98 Å, 1.88 Å, and 2.92 Å, respectively. That is in addition to the binding to the pocket active residue, ALA 162, through the relatively stronger conventional hydrogen bond at the average bond distance of 3.25 Å (Figures 7a and 7b).

3.1.3. Binding activities of metformin, vildagliptin, vildagliptin-metformin fixed dose combination and silymarin to catalase

The docked drugs including the vildagliptin-metformin conjugate (-9.1 kcal/mol), exhibited relatively higher binding affinities for catalase than metformin (the standard catalase activator) (-5.2 kcal/mol) (Table 2).

The obtained active pocket residues of catalase protein based on PrankWeb-based algorithm includedA_72, A_73, A_74, A_75, A_112, A_131, A_146, A_147, A_148, A_158, A_161, A_217, A_299, A_334, A_350, A_354, A_358, A_361, A_362, and A_365.

3.1.3.1. Binding interaction between metformin and catalase

Metformin (the standard catalase activator) binds to the highly conserved active binding pocket residues TYR 358, GLY 147, ASN 148, and HIS 75 through the conventional hydrogen bonds and the hydrophobic Pi-Cation bond at the average distances of 3.01 Å, 2.73 Å, 2.71 Å, and 3.58 Å, respectively (Figures 8a and 8b).

3.1.3.2. Binding interaction between silymarin and catalase

Silymarin binds to the active binding pocket residues VAL 73, VAL 74, ARG 354, HIS 75, PHE 161, TYR 358, ARG 112 of catalase protein through the hydrophobic Pi-alkyl bonds, Pi-Pi T-shaped bond, Pi-Pi stacked bonds, and Pi-Cation bond, respectively, at the average bond distances of 5.13 Å, 5.33 Å, 4.95 Å, 5.57 Å, 4.41 Å, 4.43 Å, and 4.97 Å, as well as ARG 72, MET 350, HIS 362, and ARG 365 through the relatively stronger conventional hydrogen bonds at the average bond distances of 3.45 Å, 4.73 Å, 2.54 Å, and 2.23 Å, respectively. That is in addition to binding to the proximal side chain residues ALA 133, PHE 153, and ALA 357 of the protein through the hydrophobic alkyl bonds at the bond distances of 4.07 Å, 4.61 Å, and 5.13 Å, respectively (Figures 9a and 9b).

3.1.3.3. Binding interaction between vildagliptin and catalase

Vildagliptin binds strongly to the active binding pocket residues TYR 358, HIS 75, and VAL 146 of catalase protein through the conventional hydrogen bonds and carbon-hydrogen bond respectively at the average bond distances of 4.36 Å, 3.23 Å, and 3.90 Å, as well as ARG 72 and PHE 334 through the hydrophobic alkyl and Pi-alkyl bond at the bond distances of 4.70 Å and 5.43 Å respectively. That is in addition to binding to the proximal side chain residue ALA 133 through the hydrophobic Pi-Alkyl bond at the distance of 4.27 Å (Figures 10a and 10b).

3.1.3.3. Binding interaction between vildagliptin-metformin conjugate and catalase

The vildagliptin-metformin conjugate binds to the highly hydrophobic active binding pocket residues VAL 74, HIS 362, PHE 334, VAL 146, TYR 358, ARG 72, and VAL 73 of catalase protein through the conventional hydrogen bonds and hydrophobic alkyl bonds at the bond distances of 2.36 Å, 2.22 Å, 5.11 Å, 4.71 Å, 4.76 Å, 4.74 Å, and 5.06 Å, respectively, in addition to binding to the proximal side chain residues ALA 357 and ALA 133 through the hydrophobic Pi-Alkyl bonds at the bond distances of 4.34 Å and 5.26 Å, respectively. The highest hydrophobicity values of interactions are concentrated around the binding involving VAL 73, ARG 72, and VAL 74 (Figures 11a and 11b).

3.1.4. Binding activities of metformin, vildagliptin, vildagliptin-metformin fixed dose combination and silymarin to glutathione reductase

All the docked drugs, except metformin (-5.2 kcal/mol), exhibited relatively higher binding affinities for glutathione reductase than oxiglutathione (-7 kcal/mol) (the standard glutathione reductase activator) (Table 2).

The active pocket residues of glutathione reductase protein based on the PrankWeb-based algorithm are: A_128, A_129, A_130, A_155, A_156, A_157, A_158, A_159, A_177, A_178, A_181, A_197, A_198, A_201, A_202, A_26, A_27, A_29, A_291, A_294, A_298, A_30, A_31, A_331, A_337, A_338, A_339, A_340, A_342, A_368, A_369, A_370, A_372, A_49, A_50, A_51, A_52, A_56, A_57, A_58, A_61, A_62, A_63, A_66, and A_67.

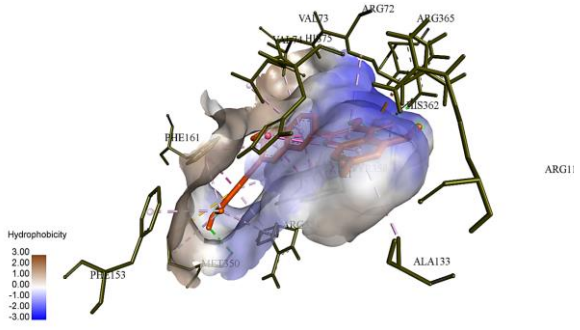

Figure 9a. Pocket hydrophobicity view of the interaction between silymarin and catalase

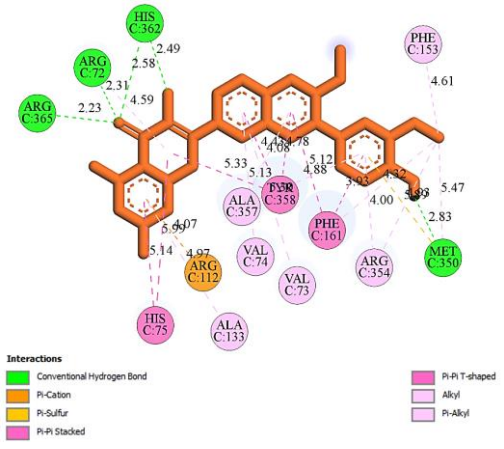

Figure 9b. Two-dimensional view of the interaction between silymarin and catalase

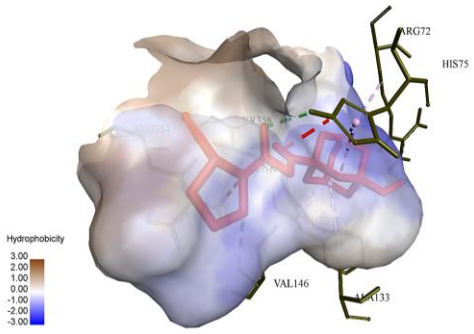

Figure 10a. Pocket hydrophobicity view of the interaction between vildagliptin and catalase

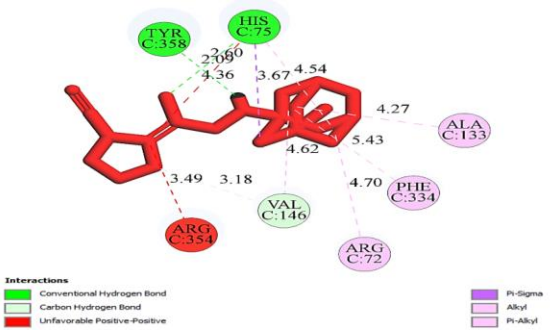

Figure 10b. Two-dimensional view of the interaction between vildagliptin and catalase

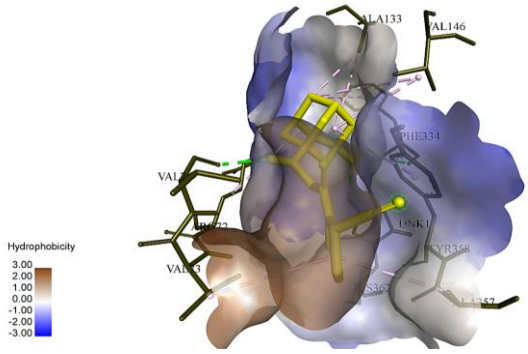

Figure 11a. Pocket hydrophobicity view of the interaction between vildagliptin-metformin conjugate and catalase

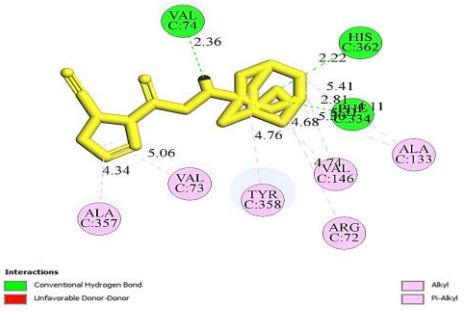

Figure 11b. Two-dimensional view of interaction between vildagliptin-metformin and catalase

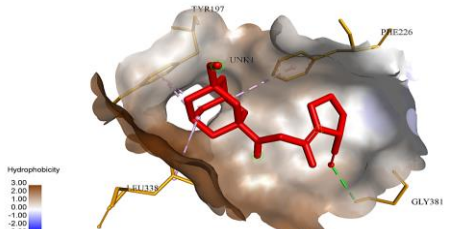

Figure 12a. Pocket hydrophobicity view of the interaction between vildagliptin and glutathione reductase

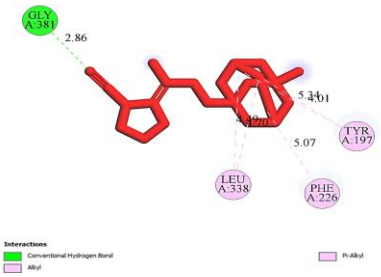

Figure 12b. Two-dimensional view of the interaction between vildagliptin and glutathione reductase

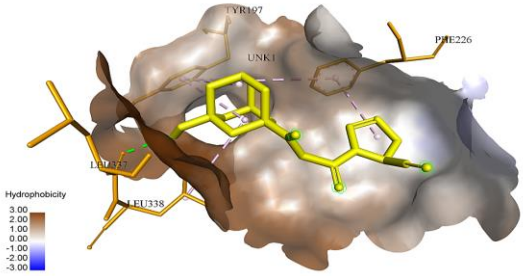

Figure 13a. Pocket hydrophobicity view of the interaction between vildagliptin-metformin conjugate on glutathione reductase

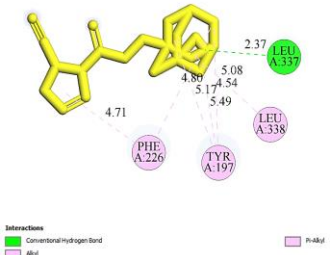

Figure 13b. Two-dimensional view of the interaction between vildagliptin-metformin conjugate and glutathione reductase

3.1.4.1. Binding interaction between vildagliptin and glutathione reductase

Vildagliptin binds to the highly conserved active binding pocket residues LEU 338 and TYR 197 of glutathione reductase through the hydrophobic Pi-alkyl bonds at average distances of 5.07 Å and 4.68 Å, respectively. That is in addition to PHE 226 and GLY 381 that bind through the hydrophobic Pi-Alkyl bond and the relatively stronger conventional hydrogen bond at the bond distances of 5.07 Å and 2.86 Å, respectively, while the highest hydrophobicity values of interactions revolve around the LEU 338 binding (Figures 12a and 12b).

3.1.4.2. Binding interaction between vildagliptin-metformin conjugate and glutathione reductase

The vildagliptin-metformin conjugate binds to the active binding pocket residues LEU 338 and TYR 197 of glutathione reductase through the hydrophobic Pi-Alkyl bonds at the average distances of 4.81 Å and 5.33 Å, respectively, as well as active LEU 337 through the relatively stronger conventional hydrogen bond at the distance of 2.37 Å. That is in addition to its binding to the hinge residue PHE 226 through the hydrophobic alkyl bond at the average distance of 4.76 Å, with the highest hydrophobicity of binding revolving around the binding of LEU 337 and LEU 338 of the target protein (Figures 13a and 13b).

3.1.4.3. Binding interaction between silymarin and glutathione reductase

Silymarin binds to the active binding pocket residues GLY 62, ILE 198, LEU 338, and PHE 372 of glutathione reductase through the hydrophobic Pi-Pi T-shaped bond, Pi-Sigma bond, Pi-Alkyl bond and Amide-Pi stacked bond respectively at the average distances of 4.98 Å, 4.40 Å, 5.16 Å, and 5.02 Å as well as the active LYS 66, VAL 370, TYR 197 and CYS 63 respectively through the relatively stronger conventional hydrogen bond at the average distances of 2.10 Å, 2.23 Å, 5.16 Å, 3.62 Å (Figures 14a and 14b).

3.1.5. Binding activities of metformin, vildagliptin, vildagliptin-metformin fixed dose combination and silymarin to vascular cell adhesion molecule-1 (VCAM-1)

All the docked compounds, excluding metformin (-4.2 kcal/mol), exhibited relatively higher binding affinities than BDBM50105195 (- 5.6 kcal/mol) (a standard VCAM-1 protein inhibitor that was validated in Phase 1 clinical trial) (Table 2). The active pocket residues of VCAM-1 protein based on the PrankWeb-based algorithm were A_136, A_155, A_156, and A_157.

3.1.5.1. Binding interaction between vildagliptin and vascular cell adhesion molecule-1 (VCAM-1)

Vildagliptin binds to the side chain residues LEU 12, GLN 14, and VAL 183 of the VCAM-1 protein through the conventional hydrogen bond, carbon-hydrogen bond, and the hydrophobic alkyl bond, respectively, at the distances of 2.16 Å, 3.54 Å, and 4.49 Å (Figures 15a and 15b).

3.1.5.1. Binding interaction between vildagliptin-metformin conjugate and vascular cell adhesion molecule-1 (VCAM-1)

The vildagliptin-metformin conjugate compound binds to the VCAM-1 protein side chain residues ARG 187 and TYR 89 through the conventional hydrogen bond at the distances of 2.84 Å and 2.25 Å; GLN 14 and ASP 17 through the carbon-hydrogen bond at the average distances of 3.63 Å and 3.78 Å respectively as well as PRO 184 and VAL 183 through the hydrophobic alkyl bond at the distances of 5.39 Å and 4.52 Å respectively (Figures 16a and 16b).

3.1.5.2. Binding interaction between silymarin and vascular cell adhesion molecule-1 (VCAM-1)

Silymarin binds to the side chain residues TYR 89 and GLN 14 of VCAM-1 protein through the conventional hydrogen bond at the distances of 2.33 Å and 2.51 Å as well as ARG 187 and ASP 94 through the hydrophobic Pi-Cation bond at the average distances of 3.99 Å and 4.91 Å. That is in addition to binding to the hinge residue PRO 184 through the Pi-alkyl bond at the average distance of 5.17 Å (Figures 17a and 17b).

3.1.6. Binding activities of metformin, vildagliptin, vildagliptin-metformin fixed dose combination and silymarin to C-X-C Chemokine Motif Receptor 1 (CXCR1)

Both vildagliptin and vildagliptin-metformin conjugate with equivalent binding affinity (-8.8 kcal/mol) exhibited relatively higher binding affinities for the chemokine interleukin-8 receptor C-X-C chemokine receptor-1 than reparixin (the standard inhibitor) (-7.9 kcal/mol) (Table 2).

The active pocket residues of CXCR1 protein based on PrankWeb-based algorithm include: A_117, A_120, A_121, A_123, A_124, A_125, A_127, A_128, A_206, A_210, A_211, A_214, A_215, A_218, A_244, A_245, A_248, A_251, A_252, A_255, A_290, A_293, A_297, A_77, A_80, and A_81.

3.1.6.1. Binding interaction between vildagliptin and CXCR1

Vildagliptin binds to CXCR1 active binding pocket residues PRO 214, MET 218, VAL 248, LEU 127, ILE 244 of CXCR1 protein through the hydrophobic alkyl bond at the average bond distances of 4.21 Å, 5.17 Å, 5.26 Å 4.41 Å, 5.23 Å as well as GLY 210 through the conventional hydrogen bond at the bond distance of 2.59 Å, with the relatively high hydrophobicity of

interactions within the active pocket condensing around the binding interactions involving VAL 248, MET 218, and PRO 214 of the target (Figure 18a and Figure 18b).

3.1.6.2. Binding interaction between vildagliptin-metformin conjugate and CXCR1

The vildagliptin-metformin conjugate compound binds to CXCR1 active binding pocket residues PRO 214, MET 218, VAL 248, LEU 127, and LEU 252 of CXCR1 protein through the hydrophobic alkyl bond at the average bond distances of 3.97 Å, 4.96 Å, 4.26 Å, 5.40 Å, 5.01 Å as well as GLY 210 through the conventional hydrogen bond at the bond distance of 2.32 Å, with the relatively high hydrophobicity of interactions within the active pocket condensing around the binding interactions involving GLY 210, MET 218, and PRO 214 of the target (Figures 19a and 19b).

Recently, the oral antihyperglycemic agent, metformin, was reported to exhibit both in vitro (Chen et al., 2013; Zhuang et al., 2022) and in vivo anticancer activities (Zakikhani et al., 2006) and protected against doxorubicin-induced toxicities through multiple mechanisms that include: increasing cleaved caspase-3 and Bax, preventing the down-regulation of Bcl-2, activating the AMPK pathway (Spiering, 2019; Chen et al., 2020; Hua et al., 2023). Thus, by reducing oxidative stress and apoptosis, as well as regulating AMPK and MAPK signaling pathways. Therefore, the results of our study are in complete agreement with these earlier reports. Doxorubicin reportedly caused AMPK activation and or Akt-mTOR pathway inhibition and culminated in autophagy disruption and pro-apoptosis, then un-degraded autolysosomes accumulation, which in turn results in ROS production and accumulation (Christidi and Brunham, 2021; Antar et al., 2023). The fact that metformin utilizes the same AMPK and mTOR pathways as doxorubicin suggests autophagy and pro-apoptosis to be parts of the protective pathways that metformin uses in ameliorating doxorubicin-mediated toxicities.

Metformin binds to the highly conserved active binding pocket residues TYR 358, GLY 147, ASN 148, and HIS 75 at the average distances of 3.01 Å, 2.73 Å, 2.71 Å, and 3.58 Å, respectively, indicating that metformin utilizes the catalase pathway for its antioxidant mechanism.

Vildagliptin has significantly attenuated doxorubicin-induced nephrotoxicity via increased iNOS and Bax positivity in doxorubicin-intoxicated renal tissues (Mostafa et al., 2021). In this study, vildagliptin showed high binding affinity for the residues MET 20, LYS 21, and ALA 24 of the Bax protein at average bond distances of 4.69 Å, 4.42 Å, and 4.28 Å, respectively; side chain residues ASN 141; LYS 137 of the caspase-3 protein through the conventional hydrogen bond at the average distances of 2.09 Å; 2.75 Å and proximal side chain residues ILE 160; LEU 136 at the average distances of 5.27 Å; 5.16 Å respectively, indicating that vildagliptin utilizes and share similar apoptotic pathway with doxorubicin. Similarly, vildagliptin strongly binds the pro-apoptotic protein, CXCR1 active binding pocket residues PRO 214, MET 218, VAL 248, LEU 127, and ILE 244 of CXCR1 protein at the average bond distances of 4.21 Å, 5.17 Å, 5.26 Å 4.41 Å, 5.23 Å, respectively, as well as GLY 210 at the bond distance of 2.59 Å, also indicating that vildagliptin utilizes the pro-apoptotic pathway to ameliorate doxorubicin toxicity.

On the pro-oxidation pathway, the fact that vildagliptin binds strongly to active binding pocket residues TYR 358, HIS 75, and VAL 146 of catalase protein through the conventional hydrogen bonds and carbon-hydrogen bond respectively at the average bond distances of 4.36 Å, 3.23 Å, and 3.90 Å, as well as ARG 72 and PHE 334 at the bond distances of 4.70 Å and 5.43 Å respectively. Also, vildagliptin binds strongly to the active binding pocket residues LEU 338 and TYR 197 of glutathione reductase at average distances of 5.07 Å and 4.68 Å, respectively, in addition to PHE 226 and GLY 381 at the bond distances of 5.07 Å and 2.86 Å, respectively, all pointing to the fact vildagliptin could be mediating its antioxidant action via the enhancement of the catalase and glutathione reductase activities.

Vildagliptin's protection against possible doxorubicin-mediated toxicities was further studied using the vascular cell adhesion molecule 1 (VCAM-1) pathway, a reliable biomarker of doxorubicin-mediated endothelial damage (Hsu et al., 2021; Afrin et al., 2022). The fact that vildagliptin strongly binds strongly to binds to the side chain residues LEU 12, GLN 14, and VAL 183 of the VCAM-1 protein at the distances of 2.16 Å, 3.54 Å, and 4.49 Å., respectively, shows that it has the potential of utilizing this pathway in eliciting its ameliorating action.

Vildagliptin-metformin conjugate strongly binds to the side chain hinge residues of MET 137 in addition to proximal side chain residues LEU 47, ALA 24, MET 20 of the Bax protein at the average bond distances of 4.58 Å, 5.27 Å, 4.73 Å, respectively, as well as LYS 21 at the average bond distance of 3.96 Å; the vildagliptin-metformin conjugate also binds to CXCR1 active binding pocket residues PRO 214, MET 218, VAL 248, LEU 127, LEU 252 of CXCR1 protein at the average bond distances of 3.97 Å, 4.96 Å, 4.26 Å, 5.40 Å, 5.01 Å, respectively as

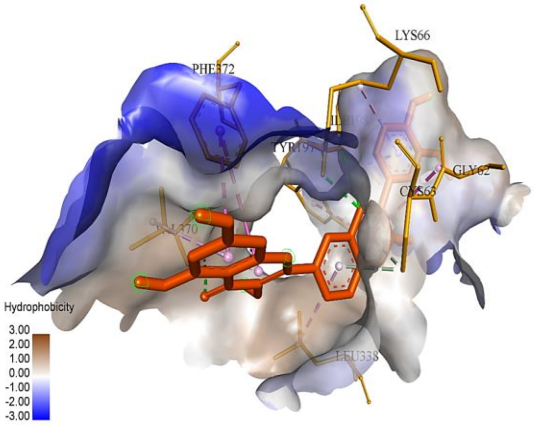

Figure 14a. Pocket hydrophobicity view of the interaction between silymarin and glutathione reductase

Figure 14b. Two-dimensional view of the interaction between silymarin and glutathione reductase

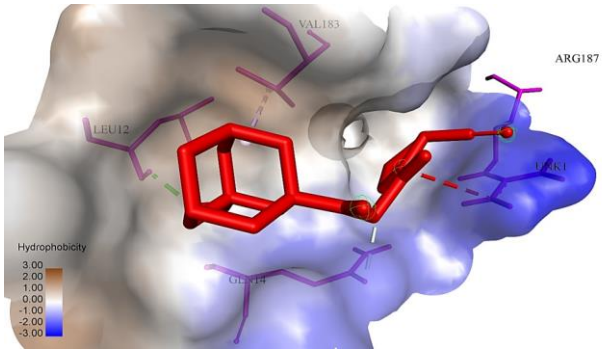

Figure 15a. Pocket hydrophobicity view of the interaction between silymarin and VCAM-1

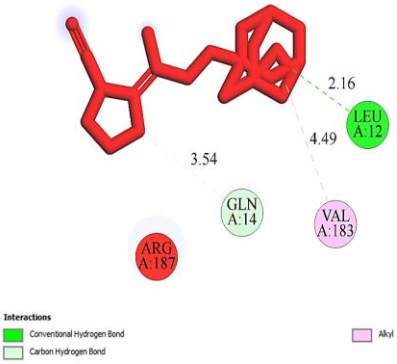

Figure 15b. Two-dimensional view of interaction between vildagliptin and VCAM-1

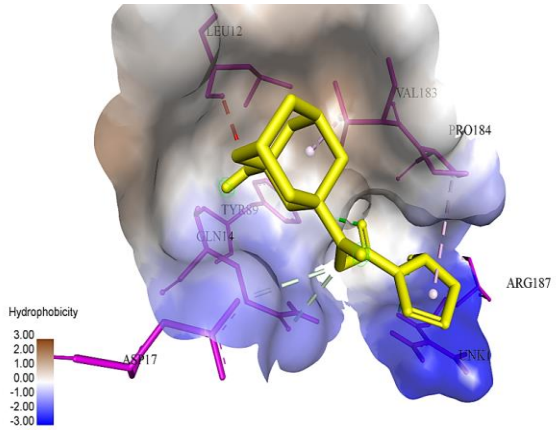

Figure 16a. Pocket hydrophobicity view of interaction between vildagliptin-metformin and VCAM-1

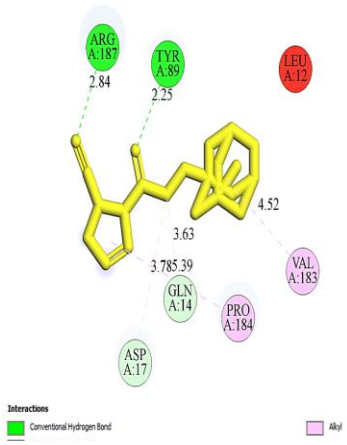

Figure 16b. Two-dimensional view of interaction between vildagliptin-metformin conjugate and VCAM-1

GLY 210 at the bond distance of 2.32 Å, with the relatively high hydrophobicity of interactions within the active pocket condensing around the binding interactions involving GLY 210, MET 218, and PRO 214 of the target. These demonstrated that vildagliptin-metformin conjugate/fixed dose combination utilizes Bax- and CXCR1-mediated pro-apoptotic pathways.

On the prooxidant pathway, vildagliptin-metformin conjugate binds to the highly hydrophobic active binding pocket residues VAL 74, HIS 362, PHE 334, VAL 146, TYR 358, ARG 72, VAL 73 of catalase protein at the bond distances of 2.36 Å, 2.22 Å, 5.11 Å, 4.71 Å, 4.76 Å, 4.74 Å, and 5.06 Å, respectively, in addition to binding to the proximal side chain residues ALA 357 and ALA 133 at the bond distances of 4.34 Å and 5.26 Å, respectively. The highest hydrophobicity values of interactions abound more around the binding involving VAL 73, ARG 72, and VAL 74. Similarly, vildagliptin-metformin conjugate binds to the active binding pocket residues LEU 338 and TYR 197 of glutathione reductase at the average distances of 4.81 Å and 5.33 Å, respectively, as well as active LEU 337 at the distance of 2.37 Å. These are in addition to its binding to the hinge residue PHE 226 at the average distance of 4.76 Å, with the highest binding revolving around the binding of LEU 337 and LEU 338 of the target protein. Thus, vildagliptin-metformin conjugate binds actively and enhances catalase and glutathione reductase activities. Also, vildagliptin-metformin conjugate binds to the VCAM-1 protein side chain residues ARG 187 and TYR 89 at the distances of 2.84 Å and 2.25 Å, respectively; GLN 14 and ASP 17 bonded at the average distances of 3.63 Å and 3.78 Å, respectively, as well as PRO 184 and VAL 183 at the distances of 5.39 Å and 4.52 Å, respectively. These results are in complete agreement with reports of other studies that showed that vildagliptin and metformin combination offered cardioprotection in ischemia-reperfusion injury mediated via antioxidant, anti-inflammatory, and Bax/Bcl2-based anti-apoptosis mechanisms as the drug combination reduced Bax and increased Bcl-2 expression (Apaijai et al., 2012; Apaijai et al., 2014).

Silymarin, an extract of milk thistle [*Silybum marianum* (L.) Gaertn.] has been reported to exhibit anticancer activities through anti-apoptosis, anti-inflammatory, and antioxidant pathways (Surai, 2015; Kim et al., 2019; Ranjan and Gautam, 2023). In this study, silymarin binds to the side chain residues, ASN 141, and LYS 137, of the caspase-3 protein at average distances of 2.09 Å, 2.75 Å, and proximal side chain residues ILE 160; LEU 136 at the average distances of 5.27 Å; 5.16 Å, respectively, with the relatively high hydrophobicity of the interactions concentrating around the ILE 160 binding, indicating its anti-apoptotic mechanism is via caspase-3 pathway.

On the pro-oxidant pathway, silymarin binds to the active binding pocket residues GLY 62, ILE 198, LEU 338, and PHE 372 of glutathione reductase at the average distances of 4.98 Å, 4.40 Å, 5.16 Å, and 5.02 Å, respectively as well as the active LYS 66, VAL 370, TYR 197 and CYS 63 at the average distances of 2.10 Å, 2.23 Å, 5.16 Å, 3.62 Å., respectively; silymarin also binds to the active binding pocket residues VAL 73, VAL 74, ARG 354, HIS 75, PHE 161, TYR 358, ARG 112 of catalase protein at the average bond distances of 5.13 Å, 5.33 Å, 4.95 Å, 5.57 Å, 4.41 Å, 4.43 Å, and 4.97 Å, respectively as well as ARG 72, MET 350, HIS 362, and ARG 365 at the average bond distances of 3.45 Å, 4.73 Å, 2.54 Å, and 2.23 Å respectively. This is in addition to binding to the proximal side chain residues ALA 133, PHE 153, and ALA 357 of the protein at the bond distances of 4.07 Å, 4.61 Å, and 5.13 Å respectively, indicating that silymarin has the affinity for utilizing the catalase and glutathione reductase pathways for its antioxidant activity.

The effect of silymarin on the VCAM-1 protein is also significant. The fact that silymarin binds to the side chain residues TYR 89 and GLN 14 of VCAM-1 protein at the distances of 2.33 Å and 2.51 Å, respectively, as well as ARG 187 and ASP 94 at the average distances of 3.99 Å and 4.91 Å as well as to the hinge residue PRO 184 at the average distance of 5.17 Å, suggests that silymarin could also mediating its effect via the VCAM-1 pathway to ameliorate doxorubicin-mediated vascular endothelial damage.

3.2.1. DPPH radical scavenging activities of metformin, vildagliptin, vildagliptin-metformin fixed dose combination, silymarin, and ascorbic acid

Metformin, vildagliptin, vildagliptin-metformin fixed dose combination, silymarin, and ascorbic acid significantly ($p<0.05$, $p<0.001$ and $p<0.0001$) inhibited DPPH radical in a concentration dependent manner (Table 3). At the concentration of 100 µg/ml, silymarin (at 83.90±0.27%, IC_{50} value of 31.87±0.31 µg/ml), vildagliptin-metformin fixed dose combination elicited the maximum %inhibition of 73.26 ± 0.05% (IC_{50} value of 44.24±0.14 µg/ml) which was relatively comparable to that of ascorbic acid (84.34 ± 0.01 %) (IC_{50} value of 29.84±0.17 µg/ml) (the standard antioxidant drug) at the same concentration (Table 3). This was followed by metformin (66.59±1.12%; IC_{50} value of 43.96±0.30 µg/ml), and vildagliptin (64.59±0.27%; IC_{50} value of 61.23±0.48 µg/ml) being the least (Table 3).

3.2.2. Antioxidant activity of of metformin, vildagliptin, vildagliptin-metformin fixed dose combination, silymarin and ascorbic acid via FRAP assay

The antioxidant activities of of metformin, vildagliptin, vildagliptin-metformin fixed dose combination, and silymarin were analyzed via FRAP assay and expressed through ascorbic acid (µg/ml). Table 4 shows that silymarin (of maximum %inhibition value of 70.35±0.10%, and IC_{50} value of 68.83±0.20 µg/ml), and vildagliptin-metformin fixed dose combination had the highest FRAP value (of maximum %inhibition value of 68.31±0.38%, and IC_{50} value of 72.04±0.43 µg/ml), while metformin showed the second highest activity (inhibition value of 62.34±0.50%, IC_{50} value of 79.07±0.49 µg/ml). The FRAP value for vildagliptin was the least (inhibition value of 52.5±0.00%, IC_{50} value of 93.72±0.38 µg/ml) (Table 4). Thus, highlighting the potent FRAP activities of silymarin and vildagliptin-metformin fixed dose combination that were comparable to that of the standard antioxidant drug, ascorbic acid (Table 4).

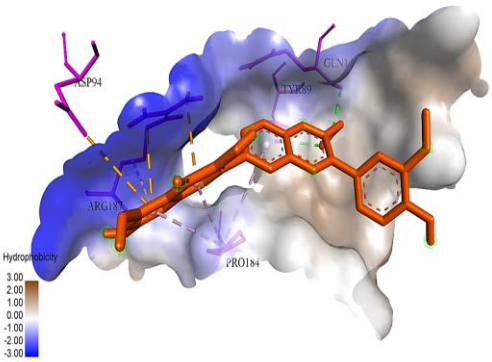

Figure 17a. Pocket hydrophobicity view of interaction between vildagliptin-metformin and VCAM-1

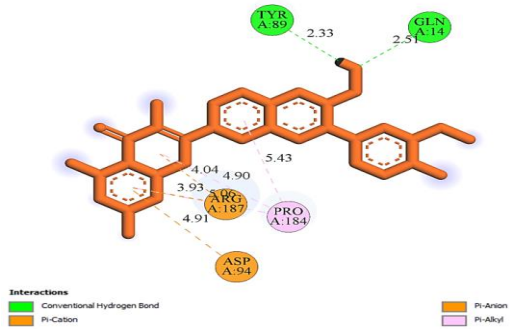

Figure 17b. Two-dimensional view of interaction between silymarin and VCAM-1

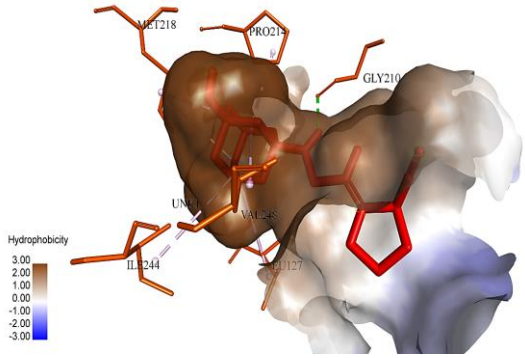

Figure 18a. Pocket hydrophobicity view of interaction between vildagliptin and CXCR1

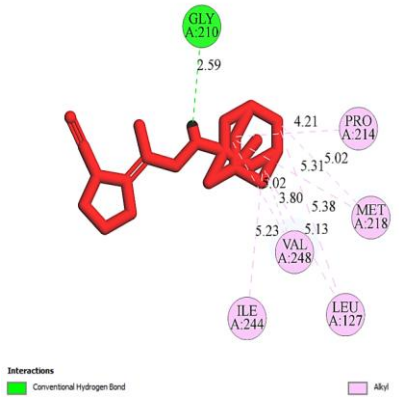

Figure 18b. Two-dimensional view of interaction between vildagliptin and CXCR1

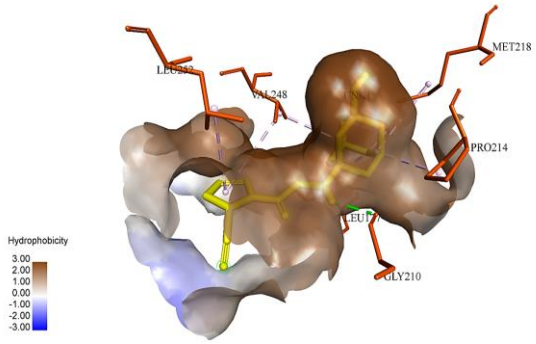

Figure 19a. Pocket hydrophobicity view of the interaction between vildagliptin-metformin conjugate and CXCR1

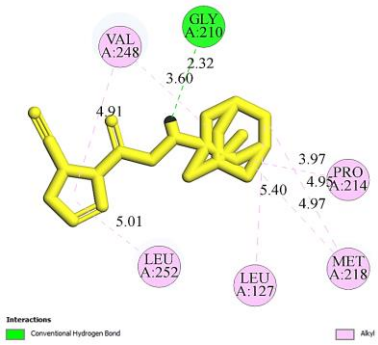

Figure 19b. Two-dimensional view of the interaction between vildagliptin-metformin conjugate and CXCR1

3.2.3. Nitrite radical scavenging activities of metformin, vildagliptin, vildagliptin-metformin fixed dose combination, silymarin, and ascorbic acid

Nitrite radical scavenging assay was carried out on the tested drugs metformin, vildagliptin, vildagliptin-metformin fixed dose combination, silymarin with ascorbic acid serving as the standard drug from a concentration of 25 to 100 µg/ml. Percentage free radical scavenging against concentration of the tested drugs as shown in Table 5. The four tested drugs exhibited varying antioxidant activity through competing with oxygen to scavenge for the nitrite radical which was generated from sodium nitroprusside (SNP) at physiological pH in an aqueous environment. The antioxidant activities of the tested drugs significantly ($p<0.05$, $p<0.001$ and $p<0.0001$) increased with increasing concentrations at between 50-100 µg/ml (Table 5). Silymarin (% inhibition of 76.88±0.12%, and IC_{50} value 48.00±0.15 µg/ml) and vildagliptin-metformin fixed dose combination (70.89 ± 0.36% , IC_{50} value of 53.34±0.43 µg/ml) demonstrated the most significant ($p<0.0001$) nitrite radical scavenging activity at 75 and 100 µg/ml concentrations, and ascorbic acid (% inhibition of 85.76 ± 0.34%, IC_{50} value of 32.53±0.36 µg/ml) followed by metformin (% inhibition of 55.40 ± 0.10%, IC_{50} value of 60.04±0.15 µg/ml) and the least being vildagliptin (% inhibition of 58.48 ± 0.22%, IC_{50} value of 62.10±0.11 µg/ml) (Table 5).

The proposed antioxidant mechanisms of metformin, vildagliptin, vildagliptin-metformin conjugate, and silymarin were collaborated by the in vitro antioxidant findings that showed all the tested drugs inhibited DPPH radical generation, suggesting free radicals scavenging activities of the drugs, with silymarin and vildagliptin-metformin conjugate exhibiting the maximal inhibitory activity. Similarly, all the test drugs exhibited antioxidant activities in the FRAP and NO assays, with silymarin and vildagliptin-metformin conjugate exhibiting the most significant antioxidant activity over its individual component drug: vildagliptin and metformin. Our result is in complete agreement with previous reports on the in vitro antioxidant activities of metformin (Manica et al., 2023), vildagliptin (Singh et al., 2021) and silymarin (Köksal et al., 2019; Azadpour et al., 2021).

4.0 Conclusion

Through the in silico and in vitro antioxidant studies conducted, this study is demonstrating for the first time the therapeutic potentials of vildagliptin-metformin conjugate, and silymarin in ameliorating doxorubicin-induced toxicities that were mediated via anti-apoptosis, antioxidant/free radical scavenging activities, and endothelial protective mechanisms. Thus, highlighting the therapeutic re-purposing potential of this fixed-dose combination in cancer chemotherapy

Acknowledgement

The authors sincerely appreciate the technical support provided by Dr. Temidayo O. Adigun of the Department of Biochemistry, University of Ilorin, Ilorin, Kwara State and Mr. Sunday O. Adenekan (Chief Technologist) of the Department of Medical Biochemistry, College of Medicine, University of Lagos, Idi-Araba, Lagos State, in the areas of molecular docking studies and in vitro antioxidant analysis, respectively.

Conflicts of Interest

The authors declare that the research was conducted in the absence of any commercial or financial relationships that could be construed as a potential conflict of interest.

Author Contributions

Conception: Adeneye A.A.
Design: Adeneye A.A.
Execution: Amuni M.A.
Data analysis & Interpretation: Adeneye A.A., Amuni M.O.
Writing the paper: Adeneye A.A., Amuni M.O.

Funding

None received from funding agencies in the public, commercial, or not-for-profit sector

References

Adebayo, S.A., Ondua, M., Shai, L.J., and Lebelo, S.L. (2019). Inhibition of nitric oxide production and free radical scavenging activities of four South African medicinal plants. Journal of Inflammation Research, 12: 195-203. https://doi.org/10.2147/JIR.S199377

Afrin, H., Huda Md.N., Islam. T.,Oropeza, B.P., Alvidez, E., Abir, M.I., Boland, T., Turbay, D., and Nurunnabi, Md. (2022). Detection of anticancer drug-induced cardiotoxicity using VCAM1-targeted nanoprobes. ACS Applied Materials & Interfaces,14(33): 37566-37576. https://doi.org/10.1021/acsami.2c13019

Agaba, A., Ebada, M., and Emara, H. (2021). Protective effect of metformin on doxorubicin-induced cardiomyopathy in the adult male Albino rats (light and electron microscopic study). Al-Azhar International Medical Journal, 2(4): 1-8. https://doi.org/10.21608/AIMJ.2021.72417.1458

Ajzashokouhi, A., Bostan, H., Jomezadeh, V., Hayes, A., and Karimi, G. (2020). A review on the cardioprotective mechanisms of metformin against doxorubicin. Human & Experimental Toxicology, 39(3): 237-248. https://doi.org/10.1177/0960327119888277

Antar, S.A., Abd-Elsalam, M., Abdo, W., Abdeen, A., Abdo, M., Fericean, L., Raslan, N.A., Ibrahim, S.F., Sharif, A.F., Elalfy, A., Hend E. Nasr, H.E., Zaid, A.B., Atia, R., Atwa, A.M., Gebba, M.A., and Alzokaky, A.A. (2023). Modulatory role of autophagy in metformin therapeutic activity toward doxorubicin-induced nephrotoxicity. Toxics, 11: 273. https://doi.org/10.3390/toxics11030273

Apaijai, N., Pintana, H., Chattipakorn, S.C., and Chattipakorn, N. (2012). Cardioprotective effects of metformin and vildagliptin in adult rats with insulin resistance induced by a high-fat diet. Endocrinology, 153: 3878-3885. https://doi.org/10.1210/en.2012-1262

Apaijai, N., Chinda, K., Palee, S., Chattipakorn, S., and Chattipakorn, N. (2014). Combined vildagliptin and metformin exert better cardioprotection than monotherapy against ischemia-reperfusion injury in obese-insulin resistant rats. PLoS ONE, 9(7):e102374. https://doi.org/10.1371/journal.pone.0102374

Asensio-López, M.C., Lax, A., Pascual-Figal, D.A., Valdés, M., and Jesús Sánchez-Más, J. (2011). Metformin protects against doxorubicin-induced cardiotoxicity: Involvement of the adiponectin cardiac system.Free Radical Biology and Medicine,51(10): 1861-1871. https://doi.org/10.1016/j.freeradbiomed.2011.08.015

Asnani, A., Zheng, B., Liu, Y., Wang, Y., Chen, H.H., Vohra, A., Chi, A., Cornella-Taracido, I., Wang, H., Johns, D.G., Sosnovik, D.E., and Peterson, R.T. (2018). Highly potent visnagin derivatives inhibit Cyp1 and prevent doxorubicin cardiotoxicity. JCI Insight,3(1): e96753. https://doi.org/10.1172/jci.insight.96753

Azadpour, M., Farajollahi, M.M., Varzi, A.M., Hashemzadeh, P., Mahmoudvand, H., and Barati M. (2021). Extraction, chemical composition, antioxidant property, and in-vitro anticancer activity of silymarin from *Silybum marianum* on Kb and A549 cell lines. Current Drug Discovery Technologies, 18(4): 511-517. https://doi.org/10.2174/1570163817666200827111127

Baroroh, U., Si. S., Biotek, M., Muscifa, Z.S., Destiarani, W., Rohmatullah, F.G., and Yusuf. M. (2023). Molecular interaction analysis and visualization of protein-ligand docking using Biovia Discovery Studio Visualizer. Indonesian Journal of Computational Biology, 2(1): 22-30. https://doi.org/10.24198/ijcb.v2i1.46322

Brand-Williams, W., Cuvelier, M.E., and Berset, C. (1995). Use of a free radical method to evaluate antioxidant activity. LWT – Food Science and Technology, 28(1): 25-30. https://doi.org/10.1016/S0023-6438(95)80008-5

Caruso, G., Privitera, A., Antunes, B.M., Lazzarino, G., Lunte, S.M., Aldini, G., and Caraci, F. (2022). The therapeutic potential of carnosine as an antidote against drug-induced cardiotoxicity and neurotoxicity: Focus on Nrf2 pathway. Molecules, 27:4452. https://doi.org/10.1016/j.crphar.2023.100153

Chelliah, R., Banan-MwineDaliri, E., and Oh, DH. (2022). Screening for antioxidant activity: nitric oxide scavenging assay. In: Dharumadurai, D. (eds) Methods in Actinobacteriology. Springer Protocols Handbooks. Humana, New York, NY. https://doi.org/10.1007/978-1-0716-1728-1_62

Chen, H.P., Shieh, J.J., Chang, C.C., Chen, T.T., Lin, J.T., Wu, M.S., Lin, J.H., and Wu, C.Y. (2013). Metformin decreases hepatocellular carcinoma risk in a dose-dependent manner: population-based and in vitro studies. Gut, 62(4): 606-615. https://doi.org/10.1136/gutjnl-2011-301708

Chen, J., Zhang, S., Pan, G., Lin, L., Liu, D., Liu, Z., Mei, S., Zhang, L., Hu, Z., Chen, J., Luo, H., Wang, Y., Xin, Y., and You, Z. (2020). Modulatory effect of metformin on cardiotoxicity induced by doxorubicin via the MAPK and AMPK pathways. Life Science, 249: 117498. https://doi.org/doi: 10.1016/j.lfs.2020.117498

Chen, Y., Shi, S., and Dai, Y. (2022). Research progress of therapeutic drugs for doxorubicin-induced cardiomyopathy.

Biomedicine & Pharmacotherapy, 156: 113903. https://doi.org/10.1016/j.biopha.2022.113903

Christidi, E., and Brunham, L.R. (2021). Regulated cell death pathways in doxorubicin-induced cardiotoxicity. Cell Death & Disease, 12(4): 339. https://doi.org/10.1038/s41419-021-03614-x

Du, X., Li, Y., Xia, Y.L., Ai, S.M., Liang, J., and Sang, P. (2016). Insights into protein-ligand interactions: mechanisms, models, and methods. International Journal of Molecular Science, 17: 144-147. https://doi.org/10.3390/ijms17020144

El Kiki, S.M., Omran, M.M., Mansour, H.H., and Hasan, H.F. (2020). Metformin and/or low dose radiation reduces cardiotoxicity and apoptosis induced by cyclophosphamide through SIRT-1/SOD and BAX/Bcl-2 pathways in rats. Molecular Biology Reports, 47(7): 5115-5126. https://doi.org/10.1007/s11033-020-05582-5

Fukuda, A., Tahara, K., Hane, Y., Matsui, T., Sasaoka, S., Hatahira, H., Motooka, Y., Hasegawa, S., Naganuma, M., Abe, J., Nakao, S., Takeuchi, H., and Nakamura, M. (2017). Comparison of the adverse event profiles of conventional and liposomal formulations of doxorubicin using the FDA adverse event reporting system. PLoS ONE, 12(9): e0185654. https://doi.org/10.1371/journal.pone.0185654

Guchu, B.M., Machocho, A.K., Mwihia, S.K., and Ngugi, M.P. (2020). In vitro antioxidant activities of methanolic extracts of Caesalpinia volkensii Harms., Vernonia lasiopus O. Hoffm., and Acacia hockii De Wild. Evidence-Based Complementary and Alternative Medicine, 2020: 3586268. https://doi.org/10.1155/2020/3586268

Hua, Y., Zheng, Y., Yao, Y., Jia, R., Ge, S., and Zhuang, A. (2023). Metformin and cancer hallmarks: shedding new lights on therapeutic repurposing. Journal of Translational Medicine, 21: 403. https://doi.org/10.1186/s12967-023-04263-8

Hsu, P-Y., Mammadova, A., Benkirane-Jessel, N., Désaubry, L., and Nebigil, C.G. (2021). Updates on anticancer therapy-mediated vascular toxicity and new horizons in therapeutic strategies. Frontiers in Cardiovascular Medicine, 2021: 694711. https://doi.org/doi: 10.3389/fcvm.2021.694711

Köksal, E., GülÇİn, I., Beyza, S., Sarikaya, Ö., and Bursal, E. (2009). In-vitro antioxidant activity of silymarin. Journal of Enzyme Inhibition and Medicinal Chemistry, 24(2): 395-405. https://doi.org/10.1080/14756360802188081

Kelleni, M.T., Amin, E.F., and Abdelrahman, A.M. (2022). Effect of metformin and sitagliptin on doxorubicin-induced cardiotoxicity in rats: Impact of oxidative stress, inflammation, and apoptosis. Journal of Toxicology, 2015: 424813. https://doi.org/10.1155/2015/424813

Kim, S.H., Choo, G.S., Yoo, E.S., Woo, J.S., Han, S.H., Lee, J.H., and Jung, J.Y. (2019). Silymarin induces inhibition of growth and apoptosis through modulation of the MAPK signaling pathway in AGS human gastric cancer cells. Oncology Reports, 42(5): 1904-1914. https://doi.org/10.3892/or.2019.7295

Lee, J., Choi, M.-K., and Song, I.-S. (2023). Recent advances in doxorubicin formulation to enhance pharmacokinetics and tumor targeting. Pharmaceuticals (Basel), 16: 802. https://doi.org/10.3390/ph16060802

Levi, M., Tzabari, M., Savion, N., Stemmer, S.M., Shalgi, R., and Ben-Aharon, I. (2015). Dexrazoxane exacerbates doxorubicin-induced testicular toxicity. Reproduction, 150(4): 357-366. https://doi.org/10.1530/REP-15-0129.

Li, XR., Cheng, XH., Zhang, G-N., and Huang, J-M. (2022). Cardiac safety analysis of first-line chemotherapy drug pegylated liposomal doxorubicin in ovarian cancer. Journal of Ovarian Research, 15: 96. https://doi.org/10.1186/s13048-022-01029-6

López-López, E., Naveja, J.J., and Medina-Franco, J.L. (2019). DataWarrior: An evaluation of the open-source drug discovery tool. Expert Opinion on Drug Discovery, 15: 13-17. https://doi.org/10.1080/17460441.2019.1581170

Manica, D., Sandri, G., da Silva, G.B., Manica, A., da Silva Rosa Bonadiman, B., Dos Santos, D., Flores, É.M.M., Bolzan, R.C., Barcelos, R.C.S., Tomazoni, F., Suthovski, G., Bagatini, M.D., and Benvegnú, D.M. (2023). Evaluation of the effects of metformin on antioxidant biomarkers and mineral levels in patients with type II diabetes mellitus: A cross-sectional study. Journal of

Diabetes &its Complications, 37(7): 108497 https://doi.org/10.1016/j.jdiacomp.2023.108497

Mostafa, R.E., Morsi, A.H., and Asaad, G.F. (2021). Anti-inflammatory effects of saxagliptin and vildagliptin against doxorubicin-induced nephrotoxicity in rats: attenuation of NLRP3 inflammasome up-regulation and tubulo-interstitial injury. Research in Pharmaceutical Sciences, 16(5): 547-558. https://doi.org/10.4103/1735-5362.323920

Olorundare, O.E., Adeneye, A.A., Akinsola, A.O., Sanni, D.A., Mamoru Koketsu, M., and Mukhtar, H. (2020). Clerodendrum volubile ethanol leaf extract: A potential antidote to doxorubicin-induced cardiotoxicity in rats. Journal of Toxicology, 2020:8859716. https://doi.org/10.1155/2020/8859716

Oyaizu, M. (1986). Studies on products of browning reaction. Antioxidative activities of products of browning reaction prepared from glucosamine. The Japanese Journal of Nutrition and Dietetics, 44(6): 307-315. http://dx.doi.org/10.5264/eiyogakuzashi.44.307

Peach, M.L., Beedie, S.L., Chau, C.H., Collins, M.K., Markolovic, S., Luo, W., Tweedie, D., Steinebach, C., Greig, N.H., Gütschow, M., Vargesson, N., Nicklaus, M.C., and Figg, W.D. (2020). Antiangiogenic activity and in silico cereblon binding analysis of novel thalidomide analogs. Molecules, 25(23): 5683. https://doi.org/ 10.3390/molecules25235683

Pérez Fidalgo, J.A., García Fabregat, L., Cervantes, A., Margulies, A., Vidall, C., Roila, F., and ESMO Guidelines Working Group. (2012). Management of chemotherapy extravasation: ESMO-EONS Clinical Practice Guidelines. Annals of Oncology, 23 (Suppl 7): vii167-173. https://doi.org/10.1093/annonc/mds294

Ranjan, S., and Gautam, A. (2023). Pharmaceutical prospects of Silymarin for the treatment of neurological patients: an updated insight. Frontiers in Neuroscience, 17: 1159806. https://doi.org/10.3389/fnins.2023.1159806

Rašković, A., Stilinović, N., Kolarović, J., Vasović, V., Vukmirović, S., and Mikov, M. (2011). The protective effects of silymarin against doxorubicin-induced cardiotoxicity and hepatotoxicity in rats. Molecules, 16: 8601-8613. https://doi.org/10.3390/molecules16108601

Renu, K., Prasanna, L.P., Vellingiri, B., and Gopalakrishnan, A.V. (2022). Toxic effects and molecular mechanism of doxorubicin on different organs - an update. Toxin Reviews, 41(2): 650-674.https://doi.org/10.1080/15569543.2021.1912099

Rivankar, S. (2014). An overview of doxorubicin formulations in cancer therapy. Journal of Cancer Research and Therapeutics,10(4): 853-858. https://doi.org/10.4103/0973-1482.139267

Satyam, S.M., Bairy, L.K., Shetty, P., Sainath, P., Bharati, S., Ahmed, A.Z., Singh, V.K., and Ashwal, A.J. (2023). Metformin and dapagliflozin attenuate doxorubicin-induced acute cardiotoxicity in Wistar rats: An electrocardiographic, biochemical, and histopathological approach. Cardiovascular Toxicology 23(2): 107-119. https://doi.org/10.1007/s12012-023-09784-8

Sheta, A., Elsakkar, M., Hamza, M., and Solaiman, A. (2016). Effect of metformin and sitagliptin on doxorubicin-induced cardiotoxicity in adult male albino rats. Human & Experimental Toxicology, 35(11): 1227-1239. https://doi.org/10.1177/0960327115627685

Singh, A.K., Yadav, D., Sharma, N., and Jin, J.O. (2021). Dipeptidyl peptidase (DPP)-IV inhibitors with antioxidant potential isolated from natural sources: A novel approach for the management of diabetes. Pharmaceuticals (Basel), 14(6): 586. https://doi.org/10.3390/ph14060586

Spiering, M.J. (2019). The mystery of metformin. Journal of Biological Chemistry, 294(17):6689-6691. https://doi.org/10.1074/jbc.CL119.008628

Surai, P.F. (2015). Silymarin as a natural antioxidant: An overview of the current evidence and perspectives. Antioxidants, 4: 204-247. https://doi.org/10.3390/antiox4010204

Tian, Z., Yang, Y., Yang, Y., Zhang, F., Li, P., Wang, J., Zhang, P., Yao, W., and Wang, X. (2020). High cumulative doxorubicin dose for advanced soft tissue sarcoma. BMC Cancer, 20: 1139. https://doi.org/10.1186/s12885-020-07663-x

Trott, O. and Olson, A.J. (2010). AutoDock Vina: Improving the speed and accuracy of docking with a new scoring function, efficient optimization and multi-threading. Journal of Computational Chemistry, 31: 455-461. https://doi.org/10.1002/jcc.21334

Van, J., Hahn, Y., Silverstein, B., Li, C., Cai, F., Wei, J., Katiki, L., Mehta, P., Livatova, K., DelPozzo, J., Kobayashi, T., Huang, Y., Kobayashi, S., and Liang, Q. (2023). Metformin inhibits autophagy, mitophagy and antagonizes doxorubicin-induced cardiomyocyte death. International Journal of Drug Discovery and Pharmacology, 2(1): 37-51. https://doi.org/10.53941/ijddp.0201004

Wang, J., Liu, S., Meng, X., Zhao, X., Wang, T., Lei, Z., Lehmann, H.I., Li, G., Alcaide, P., Bei, Y., and Xiao, J. (2024). Exercise inhibits doxorubicin-induced cardiotoxicity via regulating B cells. Circulation Research, 134: 550-568. https://doi.org/10.1161/CIRCRESAHA.123.323346

Zakikhani, M., Dowling, R., Fantus, I.G., Sonenberg, N., and Pollak, M. (2006). Metformin is an AMP kinase-dependent growth inhibitor for breast cancer cells. Cancer Research, 66(21): 10269-10273. https://doi.org/10.1158/0008-5472.CAN-06-1500

Zhuang, A., Chai, P., Wang, S., Zuo, S., Yu, J., Jia, S., Ge, S., Jia, R., Zhou, Y., Shi, W., Xu, X., Ruan, J., and Fan, X. (2022). Metformin promotes histone deacetylation of optineurin and suppresses tumour growth through autophagy inhibition in ocular melanoma. Clinical and Translational Medicine, 12(1): e660. https://doi.org/10.1002/ctm2.660

Zilinyi, R., Czompa, A., Czegledi, A., Gajtko, A., Pituk, D., Lekli, I., and Tosaki, A. (2018). The cardioprotective effect of metformin in doxorubicin-induced cardiotoxicity: the role of autophagy. Molecules, 23: 1184. https://doi.org/10.3390/molecules23051184